

Sec22b determines Weibel-Palade body length by controlling anterograde endoplasmic reticulum-Golgi transport

Ellie Karampini,¹ Petra E. Bürgisser,² Jenny Olins,¹ Aat A. Mulder,³ Carolina R. Jost,³ Dirk Geerts,⁴ Jan Voorberg^{1,5} and Ruben Bierings^{1,2}

¹Molecular and Cellular Hemostasis, Sanquin Research and Landsteiner Laboratory, Amsterdam University Medical Center, University of Amsterdam, Amsterdam; ²Hematology, Erasmus MC, University Medical Center Rotterdam, Rotterdam; ³Molecular Cell Biology, Leiden University Medical Center, Leiden and ⁴Medical Biology Amsterdam University, Medical Center, University of Amsterdam, Amsterdam and ⁵Experimental Vascular Medicine, Amsterdam University Medical Center, University of Amsterdam, Amsterdam, the Netherlands

©2021 Ferrata Storti Foundation. This is an open-access paper. doi:10.3324/haematol.2019.242727

Received: November 11, 2019.

Accepted: March 24, 2020.

Pre-published: March 26, 2020.

Correspondence: RUBEN BIERINGS- r.bierings@erasmusmc.nl

Methods

Immunoblotting

Endothelial cells were grown to confluency and lysed in NP-40 based lysis buffer (0.5% NP-40, 0.5 mM EDTA, 10 mM Tris HCl pH 7.4, 150 mM NaCl), supplemented with Complete protease inhibitor cocktail (Roche, 05056489001). Proteins were separated on a Novex® NuPAGE® 4-12% Bis-Tris gel (ThermoFisher, NP0321/NP0323) and transferred onto a nitrocellulose membrane (iBlot Transfer Stack, ThermoFisher, IB3010). Membranes were blocked with Odyssey blocking buffer (LI-COR Biosciences, Lincoln, USA, LI 927) and probed with primary antibodies and subsequently with IRDye conjugated secondary antibodies (see Supplementary Table S1). Visualization of IRDye conjugated antibodies was performed by means of LI-COR Odyssey Infrared Imaging System (LI-COR Biosciences). Blot analysis for band intensities was done in Image Studio Lite (V4.0, LI-COR Biosciences) and when needed intensities were normalized to the intensity of α -tubulin, which was used as a loading control.

Fluorescence microscopy

Immunostaining and fluorescence imaging of fixed cells was performed as previously described ¹. Immunostained cells were mounted in MOWIOL mounting medium and images were acquired using Leica SP5 or SP8 confocal microscopes (Leica, Wetzlar, Germany). Images were processed and analyzed using ImageJ (<https://imagej.nih.gov/ij/>). WPB length (major axis of cigar-shaped VWF positive structures) and TGN area (periphery of TGN46 staining) were measured as pixels and automatically converted in μm scale in ImageJ; box graphs were plotted in GraphPad Prism 8.

Secretion assay

Endothelial cells were grown in 6-well plates and cultured for 7 days prior to the experiment with regular medium replacement. Basal VWF release was determined as unstimulated secretion over 24 hours in EGM-18 medium. For histamine-induced secretion cells were pre-

incubated in release medium [RM: serum-free M199 (Thermofisher, 22340) supplemented with 0.2% (w/v) bovine serum albumin (BSA) (Merck, 112018)] for 15-30 minutes prior to stimulation. Cells were stimulated in RM medium supplemented with 100 μ M histamine (Sigma-Aldrich, H7125). Lysates were obtained in NP-40 based lysis buffer supplemented with Complete protease inhibitor cocktail. VWF levels were determined by ELISA as described previously². Secretion is expressed as relative proportion of intracellular VWF in lysates of unstimulated cells.

VWF multimer analysis

Endothelial cell lysates, produced as described in Immunoblotting, were appropriately diluted to a final concentration of 1 nM. Samples were loaded onto freshly prepared (10×10 cm, 1.5 mm) agarose gels (SeaKem® HGT(P) Agarose, Lonza, 50050) (stacking gel: 0.75% Agarose, running gel: 1.8% Agarose) and separated for approximately 3 hours at 100V and 35 mA. VWF multimers were transferred to a PVDF membrane (BIO-RAD, 162-0177) overnight. Membranes were stained with an anti-VWF-HRP antibody (see Supplemental table S1). Chromogenic visualization of HRP was achieved with DAB peroxidase substrate kit (Vector Laboratories, SK-4100). Images were analyzed using ImageJ (<https://imagej.nih.gov/ij/>) and densitometry profiles were plotted in GraphPad Prism 8.

Electron microscopy

Cells were fixed by adding double concentrated fixative to the culture dish (end concentration of fixative: 1,5% glutaraldehyde (GA) with 0.1M cacodylate buffer) and incubating for 2 hours at room temperature. After rinsing the cells 3 time with 0,1M cacodylate buffer, the cells were postfixed with 1% OsO₄/0.1M cacodylatebuffer on ice for 1 hour. Dehydration followed with a series of ethanol solutions and after that mixtures with EPON (LX112, Leadd) and ethanol 100%, and finally pure EPON. Beem capsules filled with EPON were placed on the dishes with the open face down. After EPON polymerization at 40° at the first night, followed by a day at 70°C, the beem capsules could be snapped off. 80 μ m sections parallel to the surface of the Beem capsules containing the cultured cells were

contrasted with uranylacetate and leadcitrate. Examination of the sections was done on a FEI Tecnai Twin transmission electron microscope (FEI, Eindhoven, Netherlands). Overlapping images were collected and stitched together into separate images, as previously described ³.

Immunoelectron microscopy

Cells were fixed in 2% PFA/0,2%GA/0,1M PHEM buffer at room temperature for 2 hours. Cells were scraped using a single use plastic scraper and collected in a pellet in 12% gelatin. Pellets were cut into smaller pieces of ~1 mm³ and were impregnated with 2.3M sucrose in PBS (60 min), mounted on a stub and snap frozen in liquid nitrogen. 90 µm sections were made with a Leica EM ultracryotome and were collected on grids. Grids were labeled with rabbit anti-VWF (1:1000) (see Supplemental Table S1) and stained with 10 nm PAAu gold in 1%BSA/PBS following a protocol described previously ⁴. After rinsing the sections, the grids were mounted in 0,3% uranylacetate / 2% methylcellulose solution and were examined as described above.

Data and statistical analysis

Statistical analysis was by student's t-test and using GraphPad Prism 8 (Graphpad, La Jolla, CA, USA). Significance values are shown in the Figures and in Figure legends. Data are shown as box graphs (min. to max.), as mean ± SEM or as contingency stacked bar graphs.

Supplemental References

1. Bierings R, Hellen N, Kiskin N, et al. The interplay between the Rab27A effectors Slp4-a and MyRIP controls hormone-evoked Weibel-Palade body exocytosis. *Blood* 2012;120(13):2757–2767.
2. Schillemans M, Karampini E, van den Eshof BL, et al. Weibel-Palade Body Localized Syntaxin-3 Modulates Von Willebrand Factor Secretion From Endothelial Cells. *Arterioscler Thromb Vasc Biol* 2018;38(7):1549–1561.
3. Faas FGA, Avramut MC, van den Berg BM, Mommaas AM, Koster AJ, Ravelli RBG. Virtual nanoscopy: generation of ultra-large high resolution electron microscopy maps. *J Cell Biol* 2012;198(3):457–469.
4. Peters PJ, Bos E, Griekspoor A. Cryo-immunogold electron microscopy. *Curr Protoc Cell Biol* 2006;Chapter 4:Unit 4.7.
5. Stel H V, Sakariassen KS, Scholte BJ, et al. Characterization of 25 monoclonal antibodies to factor VIII-von Willebrand factor: relationship between ristocetin-induced platelet aggregation and platelet adherence to subendothelium. *Blood* 1984;63(6):1408–1415.

Supplemental Table S1.

target	Species (isotype)	Label	Supplier	Cat.nr /clone	Application [concentration/dilution]
VWF	mouse (IgG _{2b})	-	described in ⁵	CLB-RAg20	IF [1:1000]
α-tubulin	mouse (IgG ₁)	-	Sigma-Aldrich	T9026	WB [1:1000]
VWF	rabbit	-	DAKO	A0082	ELISA [6 µg/ml]
VWF	rabbit	HRP	DAKO	A0082	WB [3µg/ml], ELISA [2 µg/ml]
Sec22b	rabbit	-	Synaptic Systems	186 003	IF [2 µg/ml], WB [1 µg/ml]
TGN46	sheep	-	Bio-Rad	AHP500GT	IF [1:1000]
Rab27A	rabbit	-	described in ¹	B2423	IF [1:100]
Slp4-a	rabbit	-	Atlas Antibodies	HPA001475	IF [1:500]
CD63	mouse (IgG ₁)	488	Sanquin	CLB-gran/12	IF [0.4 µg/ml]
Acti-stain 670	-		Cytoskeleton	PHDN1	IF [1:400]
Hoechst	-		Life Technologies	H-1399	IF [1:50]
rabbit IgG	donkey	680LT	Li-Cor	925-68023	WB [0.1 µg/ml]
mouse IgG	donkey	800CW	Li-Cor	925-32212	WB [0.1 µg/ml]
rabbit IgG	goat	AF633	ThermoFisher	A11011	IF [2 µg/ml]
mouse IgG	goat	AF568	ThermoFisher	A11004	IF [2 µg/ml]
mouse IgG	goat	AF488	ThermoFisher	A11004	IF [2 µg/ml]
rabbit IgG	chicken	AF647	ThermoFisher	A21443	IF [2 µg/ml]

Supplemental Table S2. MISSION® Library shRNAs used in this study

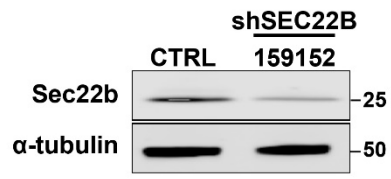
target	shRNA clone MISSION® library	shRNA target sequence
Sec22b	TRCN0000159152	GCCATCAATGAGATTTAACTT
	TRCN0000159288	GCCACAATTTGCTAACATTTA
VAMP7	TRCN0000059888	GCGAGGAGAAAGATTGGAATT
	TRCN0000059889	GCTCACTATTATCATCATCAT
	TRCN0000059890	GAGCAGATTCTGGCTAAGATA
	TRCN0000059891	GCACTTCCATATGCCATGAAT
	TRCN0000059892	CGTACTCACATGGCAATTATT
YKT6	TRCN0000059763	GCCGAAGTAGATGAGACCAAA
	TRCN0000059764	CGCATACGATGTGTCTTCCTT
	TRCN0000059765	GAGAAGCTGATCCCATGACTA
	TRCN0000059766	CGGAATGATAGTCTTGCAGGT
	TRCN0000059767	ACAGTCTAAAGCCTTCTATAA
non-targeting control (shCTRL)	-	CAACAAGATGAAGAGCACCAA

Supplemental Table S3. SEC22B gRNAs used in this study

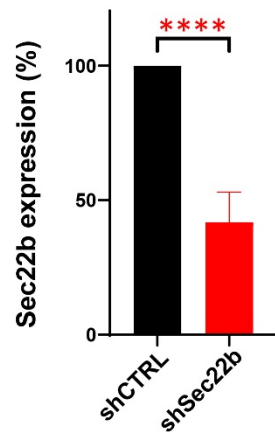
gRNA	target sequence (+PAM)	oligo	oligo sequence
gRNA1	GCTAACAATGATCGCCCGAGTGG	RBNL411	5'-caccgGCTAACAATGATCGCCCGAG-3'
		RBNL412	5'-aacCTCGGGCGATCATTGTTAGCc-3'
gRNA2	AACAATGATCGCCCGAGTGGCGG	RBNL413	5'-caccgAACAATGATCGCCCGAGTGG-3'
		RBNL414	5'-aacCCTCGGGCGATCATTGTTc-3'
gRNA3	TTCGTCTCCTGCATCGAGGCGG	RBNL415	5'-caccgTTCGTCTCCTGCATCGAGG-3'
		RBNL416	5'-aacCCTCGATGCAGGAGGACGAAc-3'

Supplemental Figure S1.

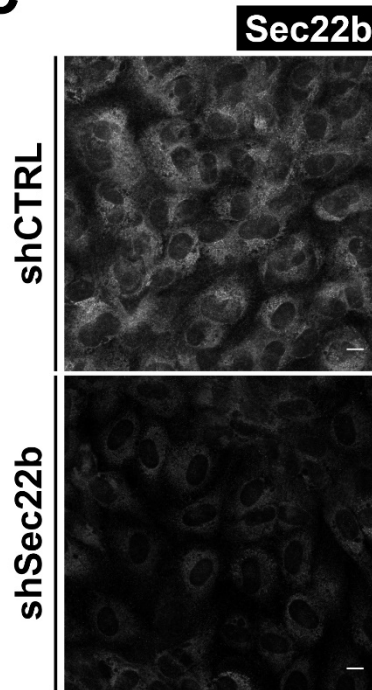
A



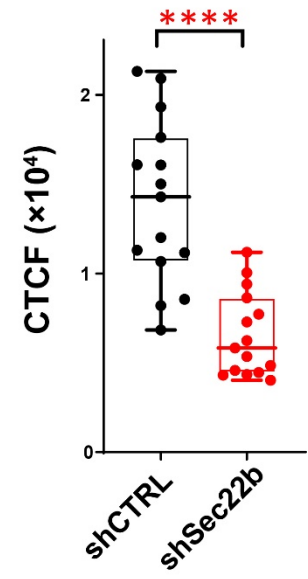
B



C

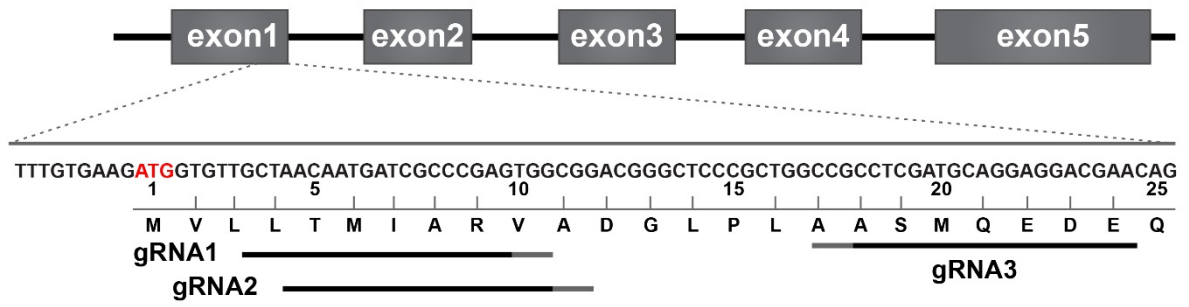


D

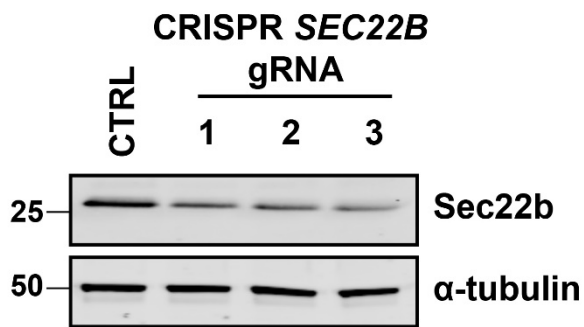


Supplemental Figure S2.

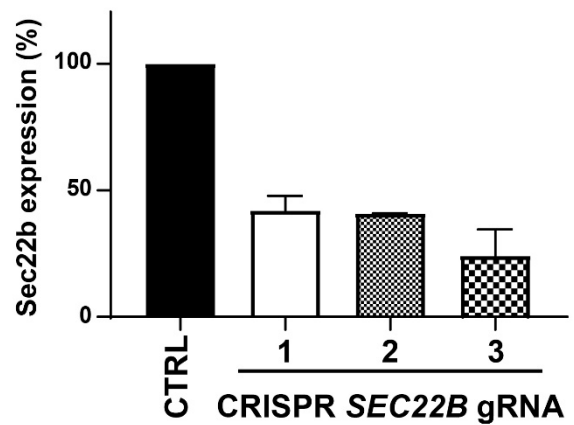
A



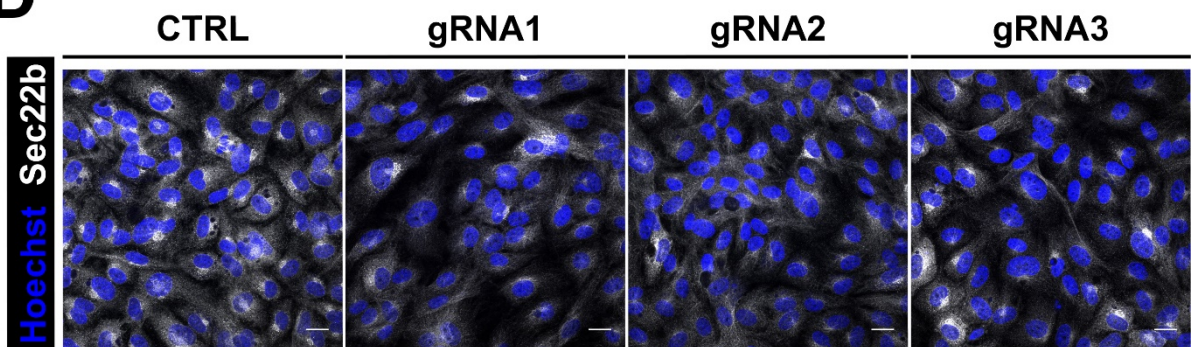
B



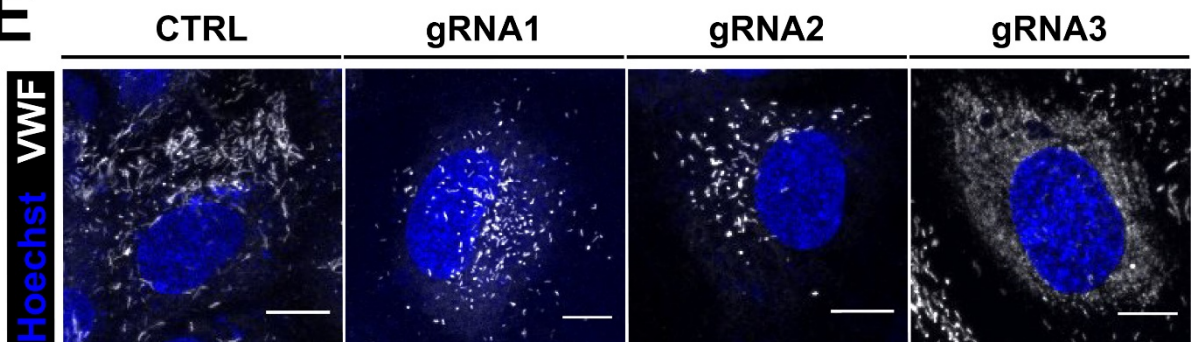
C



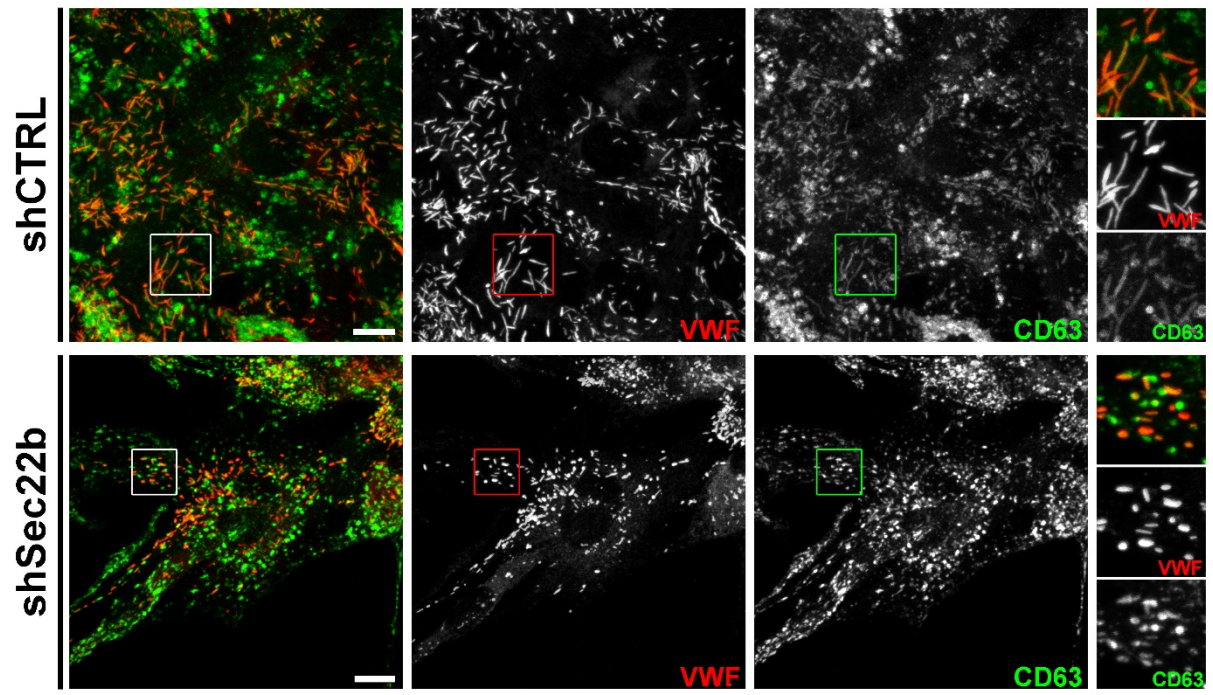
D



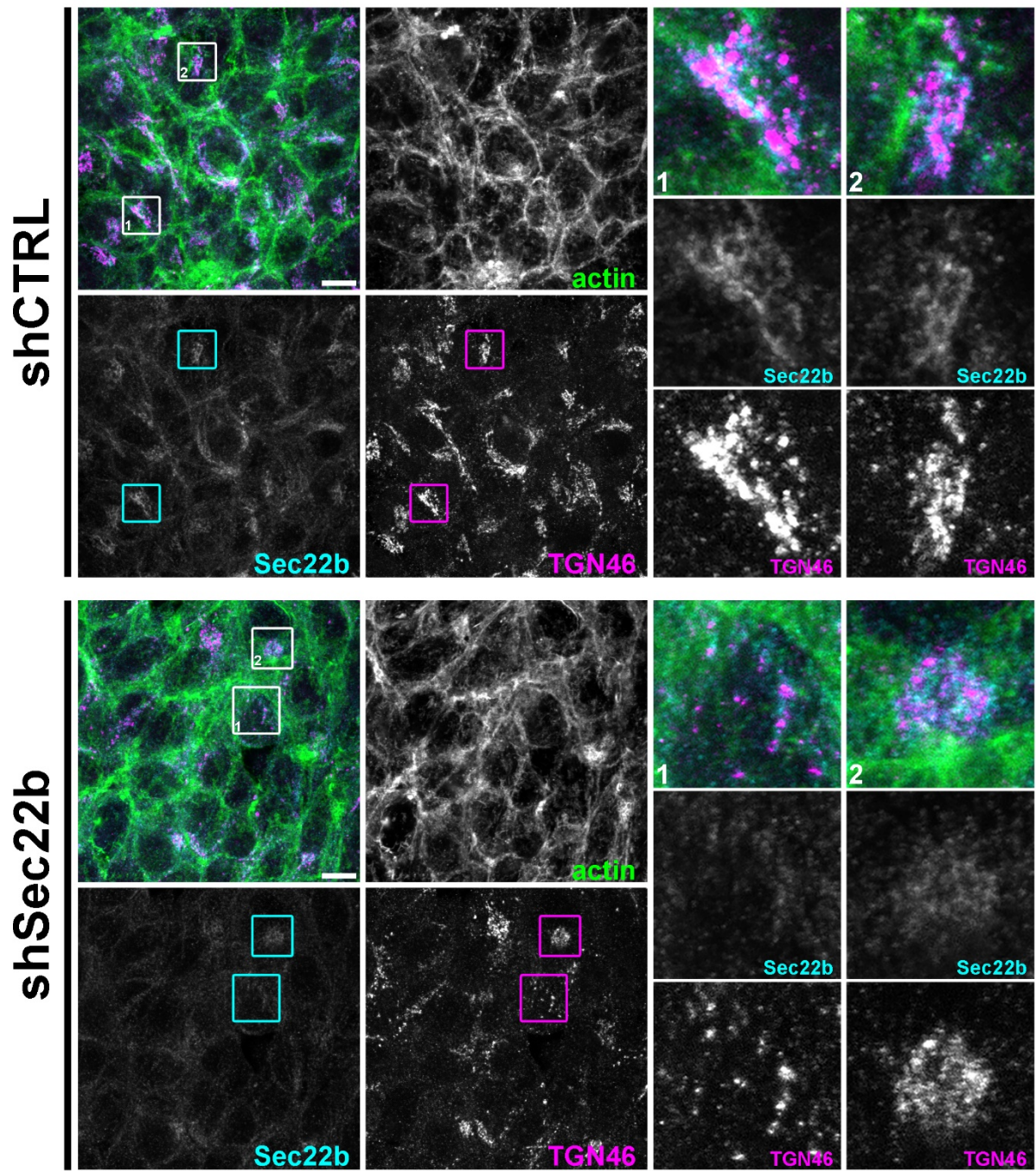
E



Supplemental Figure S3.

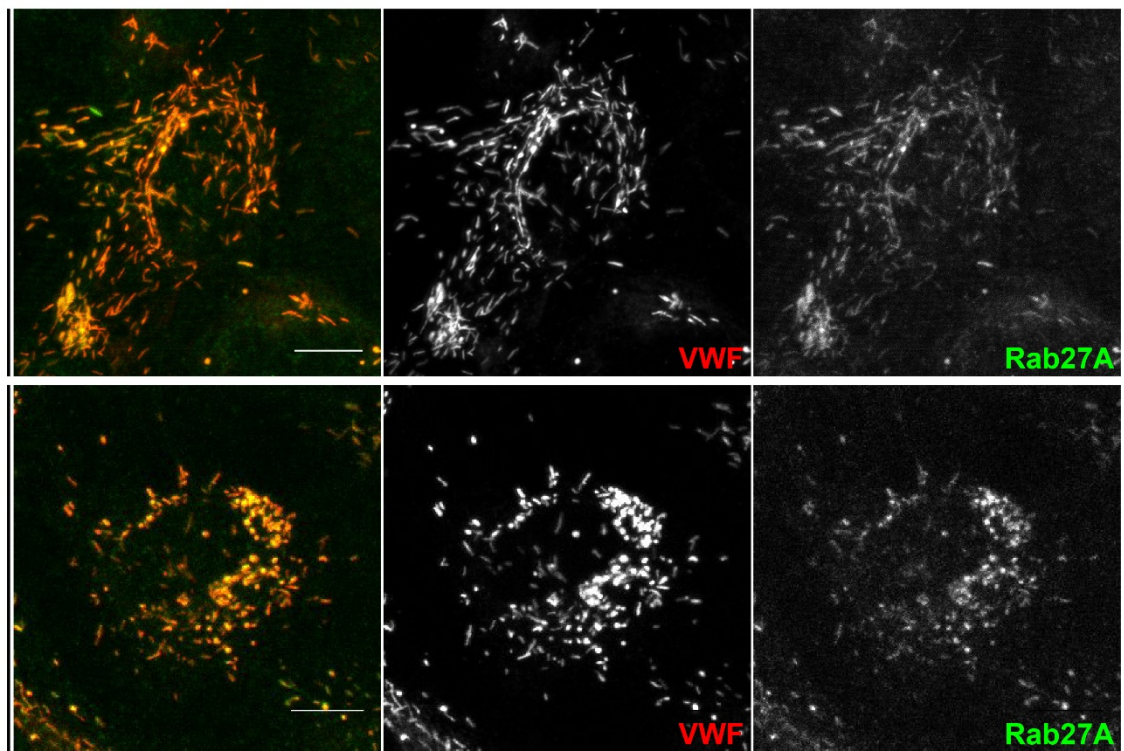


Supplemental Figure S4.

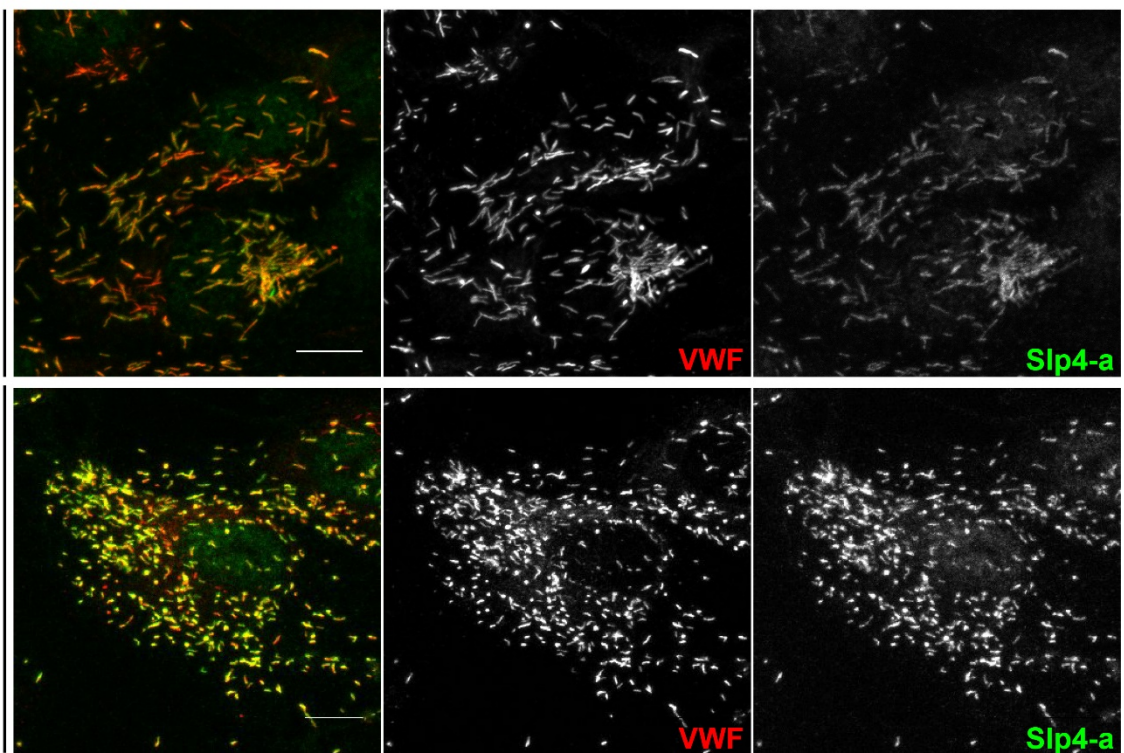


Supplemental Figure S5.

A



B



Supplemental Figure Legends

Supplemental Figure S1. shRNA silencing of Sec22b in endothelial cells. (A) Sec22b expression in HUVEC lysates after Sec22b silencing determined using immunoblotting. α -tubulin was used as a loading control. Molecular weight indicators are shown on the right in kDa. (B) Quantification of Sec22b expression in Sec22b silenced endothelial cells normalized to shCTRL treated cells. (C) Immunostaining of Sec22b in shCTRL- and shSec22b-treated HUVECs. (D) Quantification of Sec22b immunoreactivity (corrected total cell fluorescence, CTCF) in shCTRL- and shSec22b-treated cells.

Supplemental Figure S2. Analysis of bulk populations of Sec22b CRISPR-engineered HUVECs (A) Graphic representation of gRNA design at the exon 1 of *SEC22B* for CRISPR/Cas9 knock out generation. gRNAs and PAMs are indicated underneath the sequence and translated region. (B) WB analysis of Sec22b expression in control and gRNA1, 2 and 3 samples (α -tubulin as loading control). (C) Bar graph of Sec22b expression (normalized to α -tubulin) in control and CRISPR knock out cells. (D) Immunofluorescent staining of Sec22b in CTRL, gRNA1, gRNA2 and gRNA3 HUVECs (blue channel: nucleus staining). (E) Immunofluorescent staining of VWF in CTRL, gRNA1, gRNA2 and gRNA3 HUVECs (blue channel: nucleus staining).

Supplemental Figure S3. Morphology and abundance of endolysosomal organelles are not dependent on Sec22b. Immunofluorescent staining of VWF (red) and CD63 (green) in shCTRL and shSec22b HUVECs (scale bar set at 10 μ m, merge of channels on the left; magnifications of the cropped regions are shown on the right).

Supplemental Figure S4. Golgi disintegration after Sec22b silencing in HEK293T cells. Immunofluorescent staining of actin (green), Sec22b (cyan) and TGN46 (magenta) in shCTRL and shSec22b treated HEK293T cells (scale bar set at 10 μ m, merge of channels on the top left; magnifications of TGN46 positive structures in the cropped regions are

shown on the right). Note that in the few cells in which some Sec22b expression remains an intact Golgi persists, an example of which is shown in the far right magnification

Supplemental Figure S5. Maturation of WPBs is not in affected shSec22b-silenced endothelial cells. (A) Immunofluorescent staining of VWF (red) and Rab27A (green) in shCTRL and shSec22b HUVECs (scale bar set at 10 μ m, merge of channels on the left). B) Immunofluorescent staining of VWF (red) and Slp4-a (green) in shCTRL and shSec22b HUVECs (scale bar set at 10 μ m, merge of channels on the left).